# The ARF exchange factors Gea1p and Gea2p regulate Golgi structure and function in yeast

**Anne Peyroche[1], Régis Courbeyrette[1], Alain Rambourg[1] and Catherine L. Jackson[2,*]**

[1]Service de Biochimie et Génétique Moléculaire, Bat. 142, Département de Biologie Cellulaire et Moléculaire, CEA/Saclay, 91191 Gif-sur-Yvette, France
[2]Cell Biology and Metabolism Branch, NICHD, NIH, Bldg. 18T, Room 101, 18 Library Drive, Bethesda, MD 20892-5430, USA
*Author for correspondence (e-mail: cathyj@helix.nih.gov)

*Accepted 3 March 2001*
*Journal of Cell Science 114, 2241-2253 (2001)* 

## SUMMARY

**The Sec7 domain guanine nucleotide exchange factors (GEFs) for the GTPase ARF are highly conserved regulators of membrane dynamics. Their precise molecular roles in different trafficking steps within the cell have not been elucidated. We present a functional analysis of two members of this family, Gea1p and Gea2p, in the yeast *Saccharomyces cerevisiae*. Gea1p and Gea2p can functionally replace each other, but at least one is necessary for viability. Temperature sensitive *gea* mutants were generated and found to have defects in ER-Golgi and intra-Golgi transport. Similar to mutants in COPI subunits in yeast, *gea* mutants had a cargo-selective secretion defect, in that some proteins continued to be secreted whereas others were blocked in the ER or early Golgi. Like yeast *arf* mutants, the rate of transport of those proteins that continued to be secreted was slowed. In addition, the structure of Golgi elements was severly perturbed in *gea* mutants. We conclude that Gea1p and Gea2p play an important role in the structure and functioning of the Golgi apparatus in yeast.**

Key words: ADP-ribosylation factor (ARF), Guanine nucleotide exchange factor (GEF), Sec7 domain, GTP-binding protein, Brefeldin A (BFA), Trafficking, Secretory Pathway, Golgi Apparatus, Yeast

## INTRODUCTION

The small GTP-binding proteins of the ADP-ribosylation factor (ARF) family are central regulators of membrane dynamics in eukaryotic cells (Boman and Kahn, 1995; Moss and Vaughan, 1995). Like all small G proteins, ARFs exist in inactive GDP- and active GTP-bound forms. Exchange on ARF regulates its association with membranes: ARF-GDP is largely soluble with only a weak affinity for membranes, whereas ARF-GTP is tightly membrane-bound (Franco et al., 1995). ARF in its GTP-bound form activates a number of effectors, notably cytosolic coat complexes that are recruited to membranes to carry out protein sorting and to promote membrane curvature (Kirchhausen et al., 1997; Pearse et al., 2000; Schmid, 1997; Springer et al., 1999; Wieland and Harter, 1999), and lipid-modifying enzymes such as PtdIns(4)P 5-kinase (Godi et al., 1999; Honda et al., 1999). Hence ARF activation results in modulation of membrane structure and function through changes in both the protein and lipid content of the membrane on which it is localized. Spontaneous exchange of GDP for GTP on ARF occurs very slowly under physiological conditions, and hence guanine nucleotide exchange factors (GEFs) are required to activate ARF in cells. All ARF GEFs identified to date possess a protein module of approximately 200 amino acids, the Sec7 domain, so-called because it was first identified as a sequence motif in the Sec7p protein of yeast (Achstetter et al., 1988). Sec7p is localized to the Golgi complex in yeast and plays an important role in transport from the endoplasmic reticulum (ER) to and through the Golgi apparatus (Deitz et al., 2000; Franzusoff et al., 1991). The function of the Sec7 domain was elucidated when the yeast protein Gea1p, also carrying a Sec7 domain, was found in a genetic screen designed to identify an ARF GEF (Peyroche et al., 1996). The Sec7 domain of the human protein ARNO was the first to be purified and shown to have ARF GEF activity in vitro (Chardin et al., 1996). A parallel biochemical approach aimed at purifying an ARF GEF activity led to the identification of BIG1 and BIG2, mammalian orthologs of yeast Sec7p (Morinaga et al., 1997; Morinaga et al., 1996; Togawa et al., 1999). Yeast Gea1p and Gea2p belong to a distinct subfamily of ARF GEFs that also includes Golgi-localized mammalian GBF1 (Claude et al., 1999) and *Arabidopsis* GNOM (Busch et al., 1996; Shevell et al., 1994).

The first demonstration of the key role of ARF activation in membrane trafficking came from studying the in vivo effects of the fungal metabolite brefeldin A (BFA), which specifically inhibits nucleotide exchange on ARF and blocks secretion (Donaldson et al., 1992; Helms and Rothman, 1992; Klausner et al., 1992). BFA causes the Golgi to disassemble and fuse with the ER in many cell types, the TGN to fuse with the endosomal system, and lysosomes to become tubular (Hunziker et al., 1992; Lippincott-Schwartz et al., 1989; Wood and Brown, 1992). BFA also blocks specific protein transport pathways such as export of anterograde cargo from the ER (Klausner et al., 1992) and transport of the polymeric immunoglobulin receptor from the TGN to the plasma membrane (Hunziker et al., 1992; Orzech et al., 1999). We demonstrated that the major (and probably the sole) targets of

BFA in the secretory pathway of yeast are the ARF GEFs Gea1p, Gea2p and Sec7p (Peyroche et al., 1999). The yeast Gea1p and Gea2p proteins are 50% identical and functionally redundant: deletion of one or the other *GEA* gene has no effect on growth or secretion, whereas a strain lacking both genes is inviable (Peyroche et al., 1996). A fourth BFA-sensitive ARF GEF, Syt1p, has been identified in yeast, and genetic data are consistent with the idea that Syt1p is involved in transport at the TGN (Jones et al., 1999). In mammalian cells, the ARF GEF GBF1 was identified as a protein whose overexpression conferred resistance to the growth inhibition caused by BFA treatment of cells (Claude et al., 1999; Yan et al., 1994).

Although BFA has been instrumental in demonstrating the importance of sensitive ARF GEFs in membrane dynamics and protein transport, understanding the precise roles of this large family of proteins will require analysis of each individual member. Studies on Sec7p, now known to represent one sub-family of ARF GEFs, have demonstrated that this protein acts at multiple steps in transport from the ER through the Golgi apparatus, and that it is an important regulator of membrane dynamics in the ER-Golgi system of yeast (Deitz et al., 2000). In this paper we investigate the roles of the yeast Gea1p and Gea2p proteins, which belong to a sub-family distinct from that of the Sec7/BIG sub-family. We find that yeast *gea* mutants have severe defects in protein transport through the ER-Golgi system and in Golgi structure.

## MATERIALS AND METHODS

### Strains, media and materials

Yeast strains used in this study are listed in Table 1. Isolation of the *gea1-4* allele on plasmid pCLJ80 has been described (Peyroche et al., 1996). CJY054 and CJY062-10-3 are strains in which the *gea1-4* mutation has been integrated at the chromosomal *GEA1* locus. To construct these strains, the *gea1-4* gene was transferred to the integrative plasmid YIp352 *URA3*, and the resulting plasmid, pAP4, was linearized and used to transform strain CJY049-11-1. FOA-resistant derivatives were obtained and verified. CJY062-10-3 is a descendant of CJY054 obtained from crossing to an isogenic strain and sporulation of the resulting diploid. The *gea1-6* and *gea1-19* alleles were generated by random mutagenesis of plasmid pCLJ90 (*CEN-TRP1-GEA1*) followed by a screen for *gea1* temperature-sensitive mutants using an FOA-based plasmid shuffling protocol. The entire *gea1-6* and *gea1-19* open reading frames were transferred to the integrative plasmid pRS306 *URA3* to create plasmids pAP26 and pAP27, respectively. The linearized plasmids pAP26 and pAP27 were used to transform CJY049-11-4 and CJY049-11-1, respectively. The *gea1-6* integrant strain APY022 and the *gea1-19* integrant strain APY026 were obtained as described above. Yeast cultures were grown on yeast extract, peptone and dextrose (YPD; 2% Bacto-peptone (w/v), 1% yeast extract (w/v) and 2% glucose (w/v)) or synthetic minimal (SD) media supplemented as necessary (Sherman et al., 1979). Cells were grown in liquid SD media containing required supplements for metabolic labeling experiments.

### Cell labeling and immunoprecipitation

Cell labeling, immunoprecipitation and reimmunoprecipitation with secondary antisera were performed as previously described (Gaynor and Emr, 1997; Peyroche et al., 1999). Secretion of proteins into the medium was assayed as described (Gaynor and Emr, 1997; Peyroche and Jackson, 2000). Antisera against HSP150 (Russo et al., 1992), invertase (Gaynor et al., 1994), α-pheromone (Graham and Emr, 1991), CPY (Klionsky et al., 1988) and α(1,6)-mannose (Franzusoff and Schekman, 1989) have been described previously. Monoclonal antibody against ALP was from Molecular Probes Inc.

### Immunofluorescence analysis

Cultures were grown at 24°C overnight, diluted into fresh medium and grown to an $OD_{600}$ of 0.3-1.0, then either left at 24°C or shifted to 37°C. Cells were fixed by adding formaldehyde (Sigma F-1635) directly to the culture flasks to a final concentration of 3.7%. After incubation for 15 minutes at the growth temperature, cells were washed once with 1 ml of potassium phosphate buffer, then resuspended in potassium phosphate buffer containing 3.7% formaldehyde. Cells were fixed overnight at 4°C, washed once in potassium phosphate buffer, then the cell walls digested with zymolyase 40T (4 μg/μl) or 100T (200 μg/ml) in buffer containing β-mercaptoethanol (10%) for 30 minutes at 30°C. Spheroplasts were incubated with the primary antibody for 1 hour at room temperature, then with 20 μg/ml of secondary antibody (Molecular Probes Inc.) for 1 hour in the dark at room temperature. Dilutions used for the primary antibodies were as follows: purified mouse monoclonal anti-HA.11 (Babco): 1:100; 9E10 (anti-Myc mouse monoclonal, Santa Cruz): 1:10; affinity-purified anti-Anp1 (Jungmann and Munro, 1998): 1:250.

### Electron microscopy

Cells were grown in YPD medium at 24°C to an $OD_{600}$ of 0.2-0.5, centrifuged, resuspended in a small volume of YPD, then injected into 50 ml of prewarmed YPD medium in a 37°C water bath. These cultures were maintained at 37°C for 40 minutes, then glutaraldehyde added to a final concentration of 0.5%. Cells were stained, embedded and prepared for steroscopic examination as described in the accompanying article (Rambourg et al., 2001).

## RESULTS

To characterize the functions of Gea1p and Gea2p in vivo, we generated temperature-conditional mutants. Because Gea1p and Gea2p have redundant functions for growth, we isolated mutations in the *GEA1* gene in a strain carrying a deletion of *GEA2* (see Materials and Methods). We isolated three mutants, *gea1-4 gea2Δ*, *gea1-6 gea2Δ* and *gea1-19 gea2Δ*, that we will herewith designate *gea1-4*, *gea1-6*, and *gea1-19* for simplicity. The *gea1-4* allele has multiple substitutions including two in conserved regions of the Sec7 domain (Fig. 1). The *gea1-6* and *gea1-19* mutant proteins have wild-type Sec7 domains but carry lesions in the C-terminal region downstream of the Sec7 domain (Fig. 1). These mutants have different growth characteristics, with *gea1-19* having the most severe phenotype (failure to grow at 30°C and above). The *gea1-6* mutant grows well at 30°C and fails to grow at temperatures of 34°C and above. The *gea1-4* mutant has the least severe growth phenotype, growing at all temperatures up to 37°C. The *gea1-6* mutant shows synthetic interactions with the COPI subunit mutants *sec21-1* (γ-COP) and *sec27-1* (β′-COP) (data not shown), which indicates a functional interaction between Gea1p and COPI.

### Transport defects in *gea* mutants

Yeast mutants defective in subunits of COPI have a cargo-specific secretion defect (Gaynor and Emr, 1997). In *sec21-3*, defective in yeast γ-COP, certain proteins are blocked very early in transport, before exit from the ER (referred to as COPI-dependent), whereas others continue to be secreted (COPI-independent) (Gaynor and Emr, 1997). A convenient method

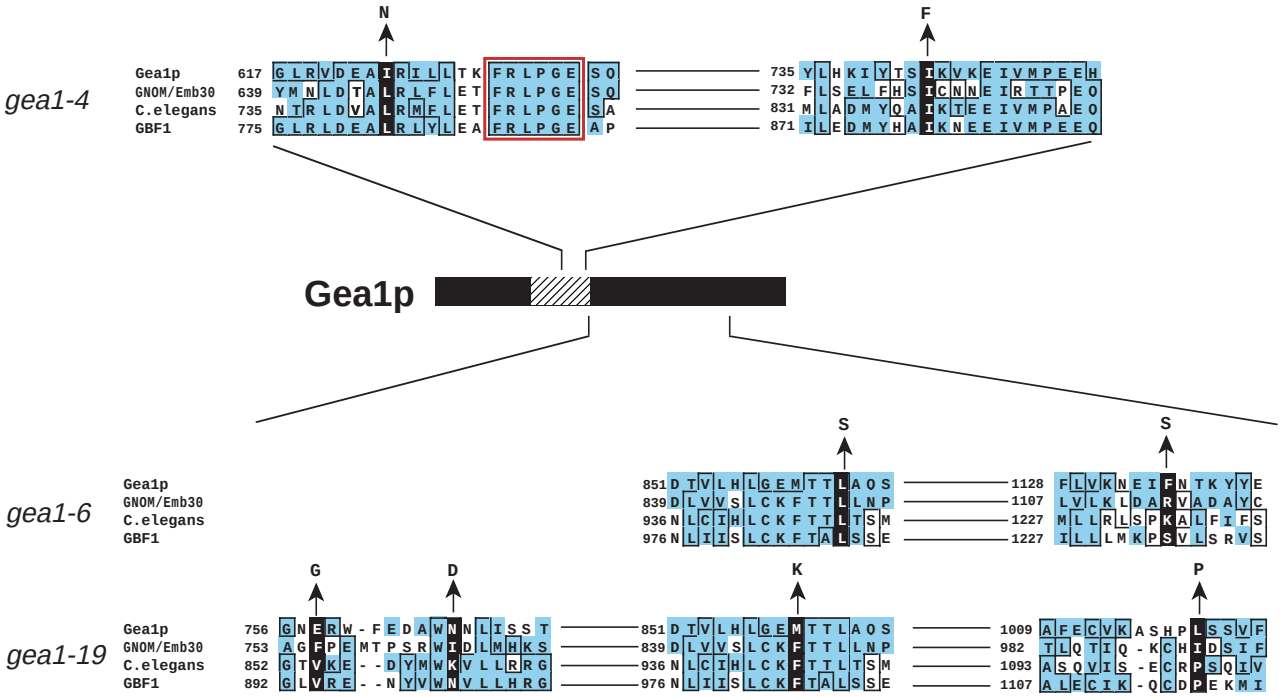


**Fig. 1.** Positions of the amino acid substitutions in the *gea1-4*, *gea1-6* and *gea1-19* alleles. Sequence alignments (with three other ARF GEFs) of the regions of Gea1p in which these changes occur are indicated. GenBank accession numbers for the sequences shown are: Gea1p (Z49531); Gnom/Emb30 (U36433); *C. elegans* ARF GEF (Z81475); and GBF1 (AF068755). The Sec7 domain of Gea1p is indicated by a striped box. *gea1-4* has additional substitutions in the C-terminal portion of the protein downstream of the Sec7 domain, but these are in poorly conserved regions of the protein. *gea1-6* has only the two substitutions shown. *gea1-19* has two additional substitutions, but only those in regions of clearly defined homology among the four ARF GEFs shown are indicated. Note that *gea1-6* and *gea1-19* both have one substitution, L862S and M859K, respectively, in the same well-conserved region. Identities in the sequence alignment are boxed, and similarities are shaded.

to assess cargo-specific secretion defects is to assay total secretion of proteins into the medium. The majority of proteins secreted by yeast cells are trapped in the periplasmic space between the plasma membrane and the cell wall, and only a small number of proteins actually escape into the surrounding medium. In *sec21-3*, transport of a subset of these media-secreted proteins is blocked at the level of the ER, whereas others are secreted normally (Gaynor and Emr, 1997). *gea* mutant strains were shifted for different lengths of time to a nonpermissive temperature for growth, then subjected to a pulse-chase regime to label cellular proteins in vivo (see Materials and Methods). All three *gea* mutants had a secretion defect resembling that of *sec21-3*. For *gea1-4*, the phenotype was less severe than that of *sec21-3*, in that secretion of COPI-dependent proteins was severely slowed, but not completely blocked (Fig. 2A). The phenotype of *gea1-19* (Fig. 2B) and *gea1-6* (not shown) was more severe than that of *gea1-4*. In these mutants, secretion was blocked for the same subset of proteins as *sec21-3*. However, unlike *sec21-3*, the rate of secretion of COPI-independent proteins was significantly

**Table 1. Strains used in this study**

| Strain | Genotype | Refs |
|---|---|---|
| RSY271 | *MATα his4-619 ura3-52 sec18-1* | Kaiser and Schekman, 1990 |
| EGY1213 | *MATα ura3-52 leu2-3,112 his3Δ200 trp1-Δ109 suc2-Δ9 sec21::HIS3/pRS315sec21-3* | Gaynor and Emr, 1997 |
| CJY052-10-2/pCLJ90 | *Matα ura3-52 leu2Δ1 his3Δ200 lys2-801 ade2-101 trp1-Δ63 gea1::HIS3 gea2::HIS3* / pCLJ90 (*CEN-TRP1-GEA1*) | Peyroche et al., 1996 |
| CJY052-10-2/pNTS6 | *Matα ura3-52 leu2Δ1 his3Δ200 lys2-801 ade2-101 trp1-Δ63 gea1::HIS3 gea2::HIS3* / pNTS6 (*CEN-TRP1-gea1-6*) | This study |
| CJY052-10-2/pNTS19 | *Matα ura3-52 leu2Δ1 his3Δ200 lys2-801 ade2-101 trp1-Δ63 gea1::HIS3 gea2::HIS3* / pNTS19 (*CEN-TRP1-gea1-19*) | This study |
| CJY049-2-3 | *MAT**a** ura3-52 leu2-3,112 his3-Δ200 ade2-101 GEA1 GEA2* | This study |
| CJY049-3-4 | *MATα ura3-52 leu2-3,112 his3-Δ200 lys2-801 ade2-101 GEA1 GEA2* | This study |
| CJY049-11-1 | *MAT**a** ura3-52 leu2-3,112 his3-Δ200 GEA1 gea2::HIS3* | This study |
| CJY049-11-4 | *Matα ura3-52 leu2,3-112 his3-Δ200 lys2-801 ade2-101 gea2::HIS3* | This study |
| CJY054 | *MAT**a** ura3-52 leu2-3,112 his3-Δ200 gea1-4 gea2::HIS3* | This study |
| CJY062-10-3 | *MATα ura3-52 leu2-3,112 his3-Δ200 lys2-801 ade2-101 gea1-4 gea2::HIS3* | This study |
| APY022 | *Matα ura3-52 leu2,3-112 his3-Δ200 lys2-801 ade2-101 gea1-6 gea2::HIS3* | This study |
| APY026 | *MAT**a** ura3-52 leu2-3,112 his3-Δ200 gea1-19 gea2::HIS3* | This study |

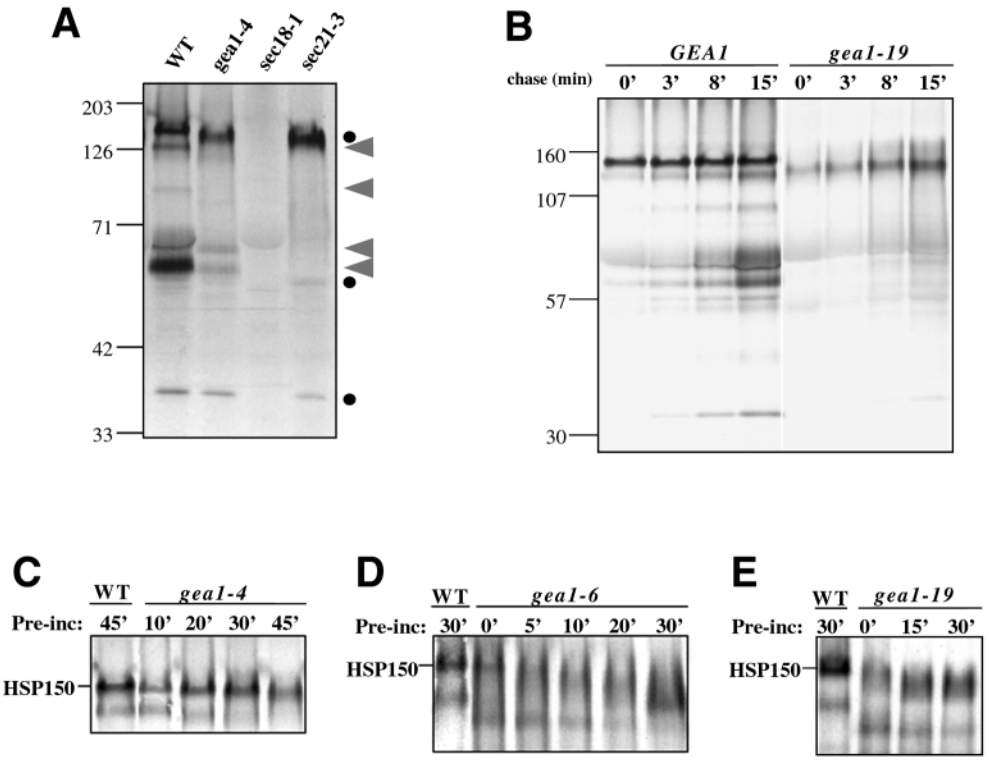


**Fig. 2.** Secretion into the medium in *gea* mutants. (A) WT (CJY049-2-3), *gea1-4* (CJY054), *sec18-1* (RSY271) and *sec21-3* (EGY1213) strains were preincubated at 38°C for 45 minutes, pulse-labeled for 10 minutes with [$^{35}$S]methionine/cysteine, then chased with non-radioactive amino acids for 30 minutes at 38°C. Proteins secreted into the medium were recovered as described in Materials and Methods, and analyzed by SDS-PAGE and fluorography. Filled circles, proteins that continue to be secreted in *sec21-3* and *gea* mutants; arrowheads, proteins whose secretion is blocked or severely retarded. (B) Wild-type strain CJY049-11-1 *GEA1* and the mutant APY026 *gea1-19* were preincubated for 20 minutes at 37°C, then pulse-labeled for 10 minutes and chased for the indicated times at 37°C. Proteins secreted into the medium were recovered and analyzed. (C) Strains CJY049-2-3 *GEA1* and CJY054 *gea1-4* were preincubated at 38°C for the times indicated, then pulse-labeled for 10 minutes and chased for 5 minutes before analyzing proteins secreted into the medium. (D,E) Strains CJY52-10-2/pCLJ90-*GEA1* and CJY052-10-2/pNTS6-*gea1-6* (D) and strains CJY52-10-2/pCLJ90-*GEA1* and CJY052-10-2/pNTS19-*gea1-19* (E) were preincubated at 37°C for the times indicated, then pulse-labeled for 10 minutes and chased for 20 minutes (D) or 30 minutes (E) prior to recovery of medium-secreted proteins.

slowed (Fig. 2B and data not shown). In addition to the selective transport defect, *sec21-3* mutants showed defects in glycosylation of those proteins that continued to be secreted, as revealed by an increased electrophoretic mobility. For the *gea* mutants, this glycosylation defect was also observed. In *gea1-4*, the defect was less severe than for *sec21-3* (Fig. 2A,C), but for *gea1-6* and *gea1-19*, the defect was even more severe than for *sec21-3* (Fig. 2B,D,E; and data not shown).

To further characterize the secretion defects in the three *gea* mutants, we carried out time courses of pre-incubation at nonpermissive temperatures for each mutant. For *gea1-4*, with increased time of preincubation at 38°C, the rate of secretion

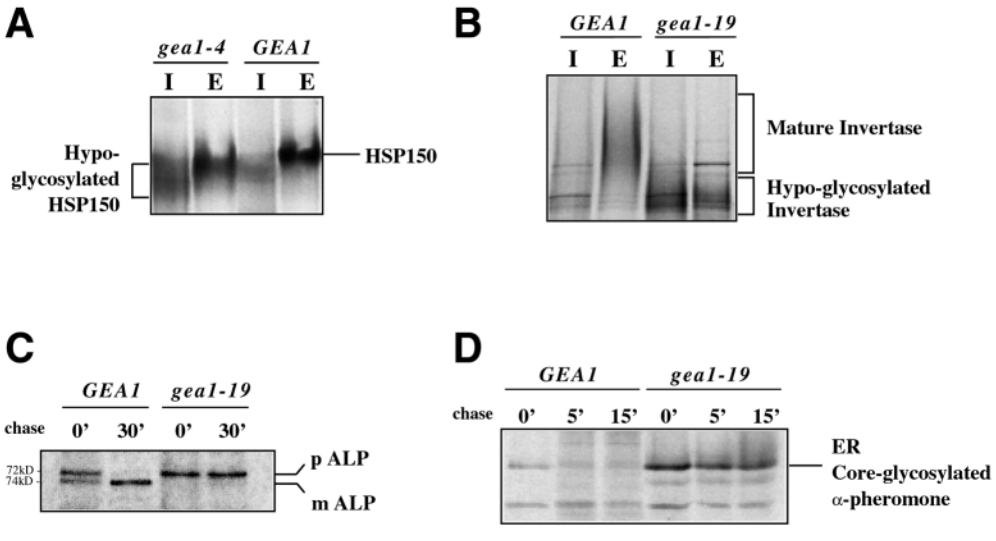


**Fig. 3.** (A) Strains CJY49-2-3 and CJY054 were preincubated for 45 minutes at 38°C, labeled for 10 minutes and chased for 30 minutes, all at 38°C. Cells and medium were separated and HSP150 immunoprecipitated using polyclonal anti-HSP150 antiserum. (B) Strains CJY52-10-2/pCLJ90-*GEA1* and CJY052-10-2/pNTS19-*gea1-19* were preincubated for 30 minutes at 37°C, labeled for 10 minutes and chased for 10 minutes, all at 37°C. Cells were then converted to spheroplasts, and internal and external fractions immunoprecipitated with antibodies against invertase. (C,D) Strains CJY52-10-2/pCLJ90-*GEA1* and CJY052-10-2/pNTS19-*gea1-19* were preincubated for 30 minutes at 37°C, labeled for 10 minutes and chased for the amount of time indicated. Cell extracts were immunoprecipitated with anti-ALP1 monoclonal antibodies (C) or with anti-α-pheromone antiserum (D), and immunoprecipitates analyzed by SDS-PAGE.

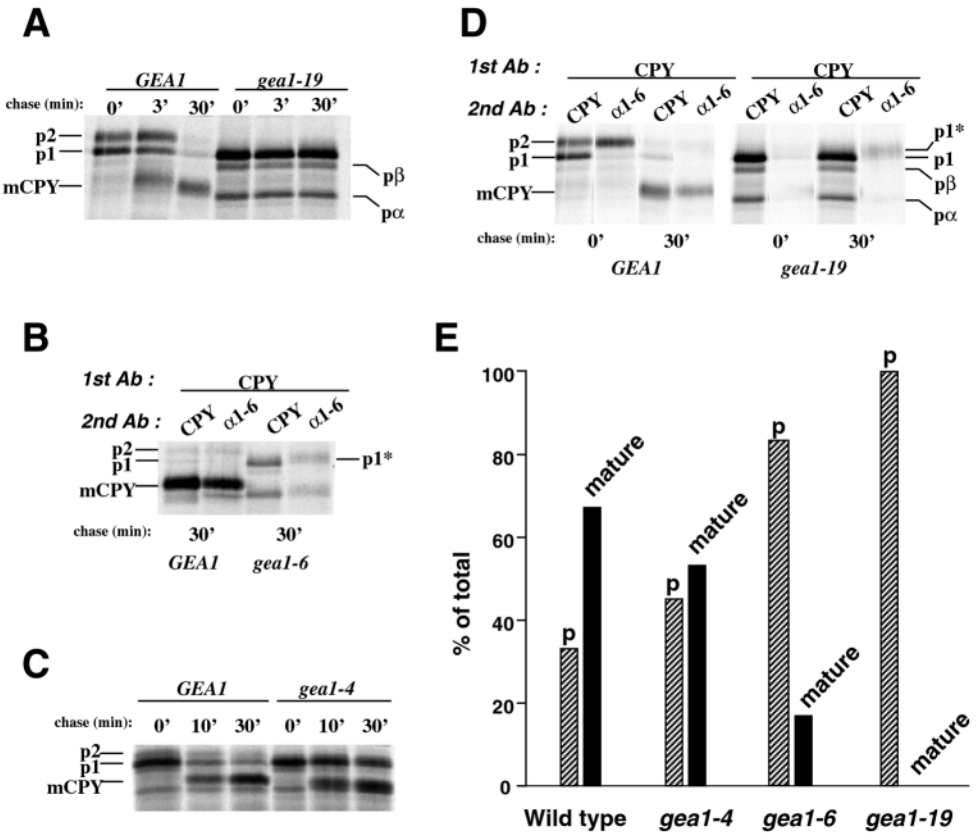


**Fig. 4.** CPY transport and maturation were monitored by pulse-chase analysis. (A) Strain APY026 *gea1-19* and wild-type strain CJY049-11-1 were incubated at 37°C for 30 minutes, pulse-labeled for 10 minutes, then chased for the times indicated. CPY was recovered from cell extracts by immunoprecipitation and visualized by SDS-PAGE and fluorography. (B) A pulse-chase regime identical to that described in part (A) was carried out for APY022 *gea1-6* and the corresponding wild-type strain (CJY049-3-4), followed by two successive immunoprecipitations, first using anti-CPY, then anti-α1,6-antisera. (C) Strain CJY062-10-3 *gea1-4* and CJY049-3-4 (wildtype) were subjected to a pulse-chase regime as described in part (A) except that preincubation was carried out at 38°C for 30 minutes. Single CPY immunoprecipitations were carried out. (D) After a first immunoprecipitation with anti-CPY antibodies as described in part (A) for strains APY026 *gea1-19* and CJY049-11-1 (*GEA1*), a subsequent immunoprecipitation was carried out using anti-α1,6-antiserum. 'mCPY' refers to the mature vacuolar form; 'p' indicates a precursor form; p1 is the ER-core-glycosylated precursor; p2 is the fully glycosylated Golgi form; pα and pβ are ER precursor forms because they do not contain α1,6-linkages. 'p1*' is a precursor form found in the *gea1* mutants that does not correspond to p1, p2 or mCPY as seen in a wild-type strain; it is a Golgi form since it is precipitated by anti-α1,6-antiserum. (E) Percentages of precursor forms (all forms grouped) and of mature vacuolar CPY for wildtype and each *gea1* mutant, as determined by quantitative Phosphorimager analysis. The values obtained for the amount of mCPY for the wild-type strain in three separate experiments were 64%, 67% and 69%: the average is shown.

of COPI-dependent proteins gradually decreased, whereas COPI-independent proteins continued to be secreted. Those proteins that continued to be secreted appeared to become progressively hypoglycosylated (Fig. 2C). The secretion defects in *gea1-6* and *gea1-19* were more severe than for *gea1-4* and were seen much more rapidly after temperature shift (Fig. 2D,E). For both mutants, even with no preincubation at 37°C, both the cargo-specific secretion block and defects in glycosylation were observed. After 30 minutes of preincubation, both mutants showed the same cargo-specific secretion block as observed for *gea1-4*, but with an even more severe hypo-glycosylation of those proteins that continued to be secreted into the medium than for *gea1-4* (Fig. 2D,E).

The highest molecular weight protein secreted into the medium is HSP150 (Gaynor and Emr, 1997; Lupashin et al., 1992; Russo et al., 1992). To examime both secreted and internal pools of HSP150, we carried out pulse-chase analysis followed by immunoprecipitation with anti-HSP150 antiserum. For wild-type cells, the majority of the protein was found in the external fraction, and ran as a relatively homogeneous band on SDS-polyacrylamide gels (Fig. 3A, lanes 3,4). In mutants *gea1-4* (Fig. 3A, lanes 1,2) and *gea1-6* (data not shown), more HSP150 was retained intracellularly compared with wildtype (Fig. 3A, compare lanes 1 and 3), which indicates a slower rate of transport. Also, for both mutants, the secreted forms were more heterogeneous in migration and migrated faster than HSP150 species secreted in the wildtype (Fig. 3A, compare lanes 2 and 4). These results confirm that the faster-migrating high molecular weight protein secreted into the medium in the *gea* mutants is indeed HSP150.

Another protein secreted in a COPI-independent fashion is invertase, which is not secreted into the medium but is trapped in the periplasm between the plasma membrane and the cell wall. After pulse-labeling cells and removal of the cell wall, both external and cell-associated fractions were immunoprecipitated with antibodies against invertase. For the wild-type strain, the majority of invertase was found in the external fraction, and migrated as a very heterogeneous band composed of forms that had undergone different levels of outerchain glycosylation (Fig. 3B). For *gea1-19*, about half of the total amount of invertase labeled in the experiment was retained intracellularly (Fig. 3B). Both the internal and external forms of invertase were severely hypoglycosylated (Fig. 3B). Similar results were obtained for *gea1-6* (data not shown). The pattern of species obtained in this experiment is characteristic of Golgi forms of invertase, and not the core-glycosylated ER forms, which run as discrete bands. To confirm that invertase produced by the *gea* mutants had received Golgi enzyme modifications, secondary immunoprecipitations using anti-α(1,6)-mannose antibodies were carried out. Addition of

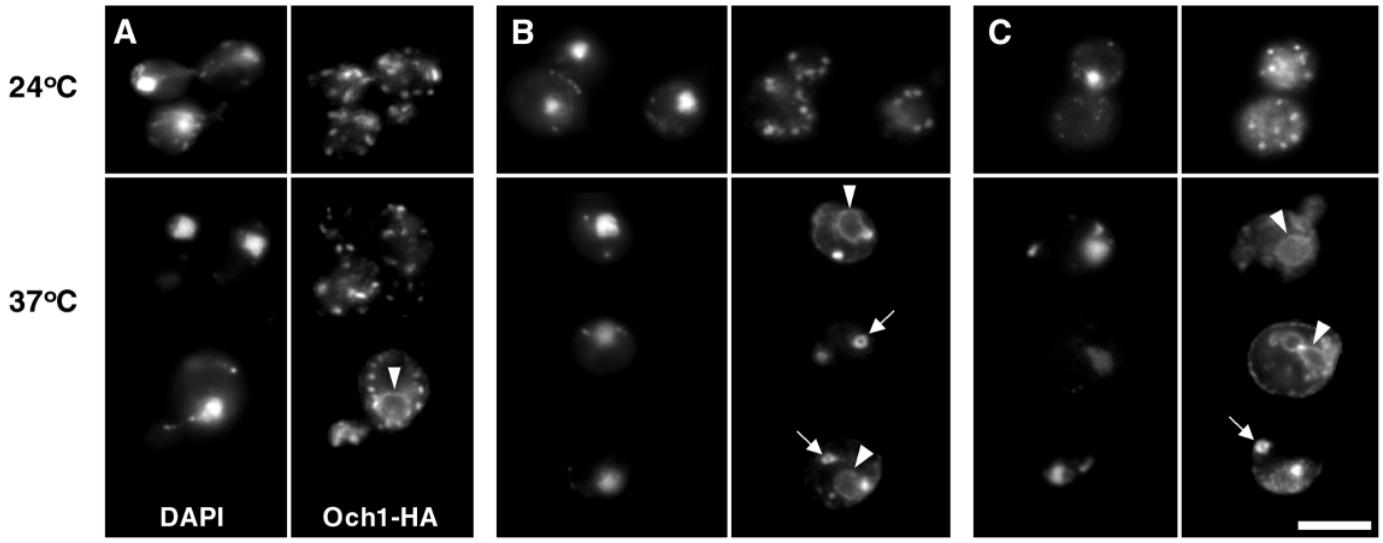


**Fig. 5.** Localization of Och1-HA in wildtype and *gea* mutant strains. The wild-type strain CJY49-3-4 (A), strain CJY62-10-3 *gea1-4* (B) and strain APY022 *gea1-6* (C), each carrying plasmid pOH (Och1-HA), were grown at 24°C, and either shifted to 37°C for 40 minutes, or left at 24°C. Cells were fixed and prepared for immunofluorescence analysis using monoclonal anti-HA antibodies. Left panels, DAPI staining to visualize nuclei; right panels, anti-HA. Arrows indicate ring-like structures and arrowheads ER/nuclear envelope staining. Bar, 5 μm.

α(1,6)-mannose linkages is performed by enzymes exclusively localized to the Golgi, and hence the presence of α(1,6)-mannose is diagnostic of transport to the Golgi apparatus in yeast. The hypoglycosylated forms of invertase were all immunoprecipitated by α(1,6)-mannose, which indicates that they are indeed Golgi forms (data not shown).

We next examined the fates of three proteins whose transport is blocked in exit from the ER in COPI mutants: the vacuolar enzyme alkaline phosphatase (ALP), the secreted protein α-pheromone and the vacuolar hydrolase carboxypeptidase Y (CPY). Transport of ALP to the vacuole was completely blocked in the *gea1-19* mutant (Fig. 3C), which indicates a block to transport at either the ER or within the Golgi. For α-pheromone, there was also a severe inhibition of secretion in the *gea1-19* mutant strain, with marked accumulation of the core-glycosylated ER form (Fig. 3D).

To further characterize the nature of the transport block in different *gea* mutants, we examined the transport of CPY in detail. The *gea1-19* mutant exhibited a total block to transport of CPY to the vacuole (Fig. 4A). A severe transport defect was also observed for *gea1-6*, although a small amount of mature vacuolar form was detected (Fig. 4B). In the *gea1-4* mutant, transport of CPY was slowed but not blocked (Fig. 4C), even after 45 minutes of preincubation at 38°C. The nature of the CPY precursors accumulated in the *gea1-6* and *gea1-19* mutants was examined by immunoprecipitation with antibodies against α(1,6)-mannose. As described above, addition of mannose via an α(1,6) linkage is diagnostic of transport to the Golgi apparatus in yeast. In *gea1-19*, the major precursor form accumulated was the p1 form, the majority of which was not precipitated by anti-α(1,6)-mannose antibodies, and hence represents an ER precursor form (Fig. 4D). A heterogeneously migrating species (p1*) of molecular weight intermediate between the ER p1 and Golgi p2 forms was observed that was precipitated by anti-α(1,6)-mannose antibodies, which indicates that it represents a form in transit through the Golgi apparatus (Fig. 4D). This form was also detected in *gea1-6* mutant cells held at the restrictive temperature of 37°C (Fig. 4B). In addition to these forms, two precursor forms were observed (pα, pβ): they represent pre-Golgi precursors as they were not precipitated by anti-α(1,6)-mannose antibodies (Fig. 4D). The CPY form that accumulated in the *gea1-4* mutant, which we assumed to be the mature vacuolar species, migrated more quickly than mature CPY in wild-type cells. To verify that this form was present in the vacuole, we repeated the pulse-chase analysis in strains lacking the vacuolar hydrolase Pep4p that cleaves the N-terminal segment of pro-CPY to give rise to the mature form. In the *GEA1 GEA2 pep4* strain, the uncleaved p2 form accumulates and, in *gea1-4 pep4*, the presumed mature form did not accumulate, indicating that it does indeed arise as a result of Pep4-dependent cleavage (data not shown). The faster migration of this mature form is probably caused by a defect in glycosylation. Hence each of the *gea* mutants affects transport of CPY to the vacuole to different extents, with *gea1-4* having the mildest phenotype, *gea1-6* a much more severe phenotype, but still allowing a small amount of transport to a Pep-4p-containing compartment, and *gea1-19* showing a complete block of transport of CPY to the vacuole (Fig. 4E).

### Localization of Golgi enzymes in *gea* mutants

Because Golgi function is severely perturbed in *gea* mutants, we examined the structure of Golgi elements, first by immunofluorescence analysis using antibodies against well-characterized Golgi proteins. Och1p is the initiating α(1,6)-mannosyltransferase in yeast, which adds the first mannose residue to the core oligosaccharides that proteins receive in the ER. Hence Och1p is the first enzymatic activity of the cis-Golgi of yeast (Dean, 1999). We examined the localization of Och1-HA, an epitope-tagged version whose function is indistinguishable from the wild-type protein (Harris and Waters, 1996), using anti-HA antibodies. The fluorescence pattern obtained for wild-type cells is characteristic of that for Golgi markers in yeast, numerous spots scattered throughout

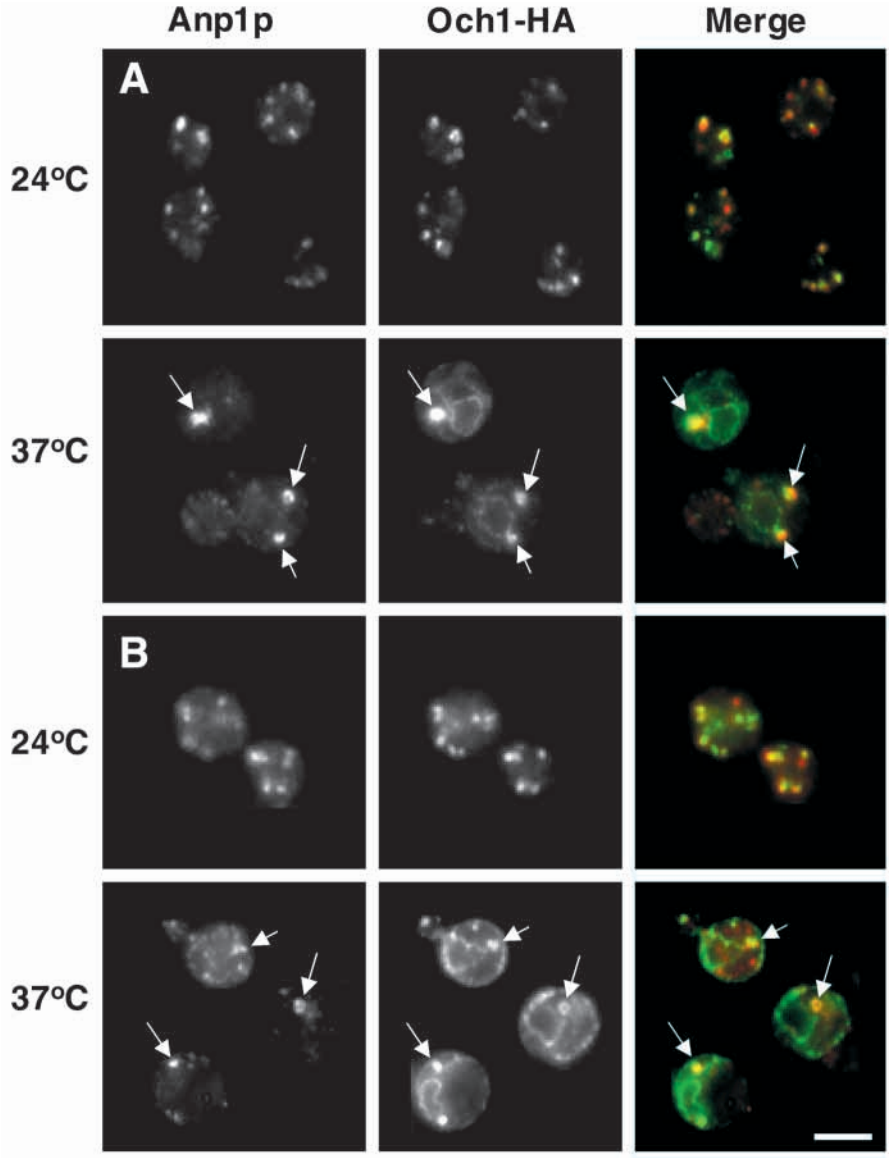


**Fig. 6.** Localization of Anp1p and Och1-HA in *gea* mutants. Strains CJY62-10-3 *gea1-4*/pOH (A) and APY022 *gea1-6*/pOH (B) were grown at 24°C, and either shifted to 37°C for 40 minutes, or left at 24°C. Cells were fixed and prepared for immunofluorescence analysis using rabbit affinity-purified anti-Anp1p antiserum and mouse monoclonal anti-HA antibodies. Arrows indicate ring-like structures. Bar, 5 μm.

the cytoplasm, both at 24°C and at 37°C (Fig. 5A). In addition to this typical pattern, after 40 minutes of incubation at 37°C, a minority of wild-type cells of our strain background (on average about 5-10%) showed a faint ER/nuclear envelope pattern (Fig. 5A). It has been noted previously that expression of *S. cerevisiae* Och1-HA in certain *S. cerevisiae* strains and in the yeast *Pichia pastoris* results in weak staining of the ER/nuclear envelope in some cells (Rossanese et al., 1999). In *gea1-4*, *gea1-6* and *gea1-19* cells incubated at 24°C, the Och1-HA pattern was very similar to that of wildtype, with numerous spots scattered throughout the cytoplasm (Fig. 5B,C; and data not shown). After 40 minutes at 37°, the *gea* mutants had very different patterns. In *gea1-4* cells, there were significantly fewer spots per cell (approximately three- to fourfold less), and the majority of cells (70-90%) contained large, ring-like structures that fluoresced more intensely than in wild-type cells or than in the control at 24°C (Fig. 5B). Even after only 15 minutes at 37°C, the number of spots per cell was reduced and many were in the form of intensely fluorescent rings. After 15 minutes at 37°C, *gea1-6* cells had five- to ten-times fewer spots of the same or greater fluorescence intensity than wild-type cells, with ring-like structures apparent in 40% of cells. In approximately 30% of cells, only diffuse staining was observed and, in approximately 70% of cells, there was a strong perinuclear pattern observed, indicating the presence of Och1-HA in the ER/nuclear envelope. After 40 minutes at 37°C, very similar results were obtained except that the ER/nuclear envelope staining was more intense (Fig. 5C). There was also an increase (to approximately 50%) of cells with diffuse fluorescence, and a decrease (to at most 30%) of cells with large ring-like structures (Fig. 5C). The *gea1-19* mutant incubated for 40 minutes at 37°C had a phenotype similar to that of *gea1-6* except that more cells exhibited a diffuse staining and fewer possessed brightly fluorescent structures. Approximately the same percentage of cells had ER/nuclear envelope staining as for the wildtype, but in some cells this staining was more intense (data not shown).

The cis-Golgi enzyme Anp1p acts downstream of Och1p, and is part of a large complex whose primary function is α1,6-mannose elongation of N-linked glycan chains (Chapman and Munro, 1994; Dean, 1999; Jungmann and Munro, 1998). We examined the localization of Anp1p by immunofluorescence in the *gea* mutants. In *gea1-4*, after 40 minutes at 37°C, there was a decrease in the number of spots compared with the 24°C control, with a corresponding increase in size and fluorescence intensity (Fig. 6A, left panels). The majority of these brightly fluorescing spots were seen to be ring-like structures at higher magnifications, as was the case for Och1-HA, with 70-80% of cells having at least one such structure (Fig. 6A). In *gea1-6*, 60-70% of cells had a diffuse staining for Anp1p, and the remainder had fewer spots per cell than the 24°C control (Fig. 6B, left panels). Approximately 30% of cells had large ring-like structures. To determine whether Och1-HA and Anp1p were in the same or distinct structures in the *gea* mutants, we carried out co-localization experiments. In wild-type cells, *gea2Δ* cells, and both *gea1-4* and *gea1-6* mutants at permissive temperature, there was a significant level of co-localization of Anp1p and Och1-HA spots (Fig.6; and data not shown). In *gea1-4* cells (and the minority of *gea1-6* cells having brightly fluorescing spots or rings), Anp1p and Och1-HA colocalized in the same ring-like structures (Fig. 6). In *gea1-4* and *gea1-6*

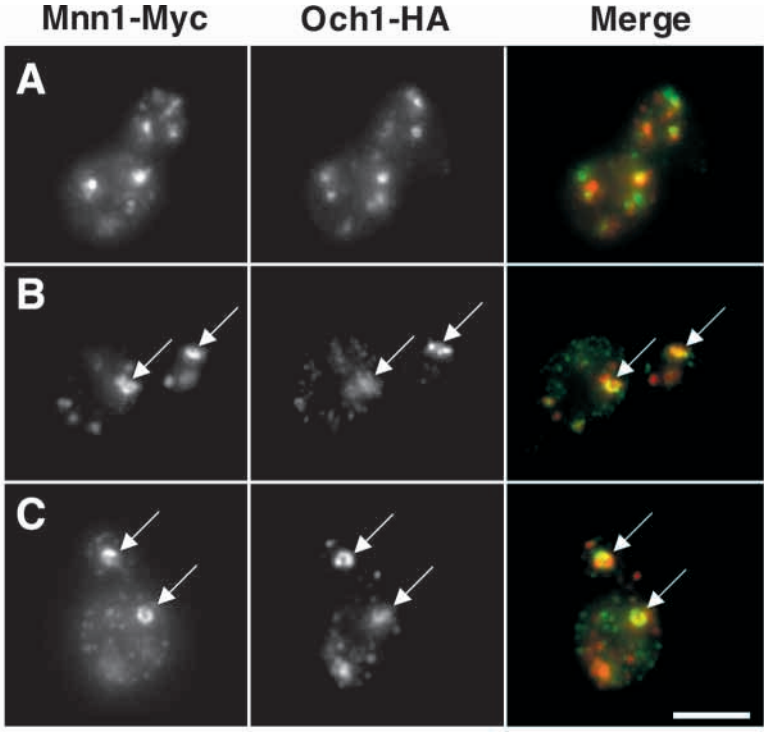


**Fig. 7.** Localization of Mnn1-Myc and Och1-HA in *gea1-4*. Strain CJY62-10-3 *gea1-4*/pOH was grown at 24°C (A) or at 37°C for 15 minutes (B) or 40 minutes (C). Cells were fixed and prepared for immunofluorescence using rabbit anti-HA antibodies and mouse anti-Myc monoclonal antibodies. Arrows point to the ring-like structures that contain both Mnn1-Myc and Och1-HA. Bar, 5 μm.

cells, where Och1-HA was present in the ER/nuclear envelope and in spots, there was colocalization of the two proteins in the spots, but no Anp1 co-localized with Och1-HA in the ER (Fig. 6).

The late-Golgi enzyme Mnn1p is an α(1,3)-mannosyltransferase that is localized at steady-state to the medial and trans compartments of the yeast Golgi (Dean, 1999; Graham et al., 1994). We used cells that expressed a Myc-tagged version of Mnn1p, from a low-copy centromeric vector, and visualized the protein using antibodies agains the Myc epitope. In wild-type cells after 15 or 40 minutes of incubation at 37°C, we observed a weak signal in the ER/nuclear envelope in about 20% of cells (data not shown). The intensity of this fluorescence was slightly higher than for Och1-HA. For the *gea1-4* and *gea1-6* mutants, the patterns observed were similar to those seen with Och1-HA (Fig. 7; and data not shown). The majority of *gea1-4* mutant cells had 1-3 ring-like structures per focal plane, whereas *gea1-6* had fewer cells with this pattern and many cells with diffuse staining or an ER/nuclear envelope pattern (Fig. 7B,C; and data not shown). In wild-type cells, there is only partial overlap in patterns between early Golgi markers such as Och1p and late-Golgi markers such as Mnn1p. For *gea1-4* at permissive temperature, we obtained similar results: only partial overlap in Och1-HA- and Mnn1-Myc-positive spot patterns (Fig. 7A). For both *gea1-4* and *gea1-6*, we observed that the brightly-fluorescing spots and ring-like structures contained both Och1-HA and Mnn1-Myc (Fig. 7B,C). In *gea1-6* cells with ER/nuclear envelope staining, we observed co-localization of Och1-HA and Mnn1-Myc in the ER/nuclear envelope (data not shown).

To detemine whether *gea* mutants have defects in the structure of endosomal compartments, we examined uptake of FM 4-64, a lipophilic dye that is internalized by yeast cells and follows the endocytic pathway to the vacuole (Vida and Emr, 1995). In both *gea1-4* and *gea1-6* mutants, the time course of uptake of the dye into dot-like endocytic structures was not

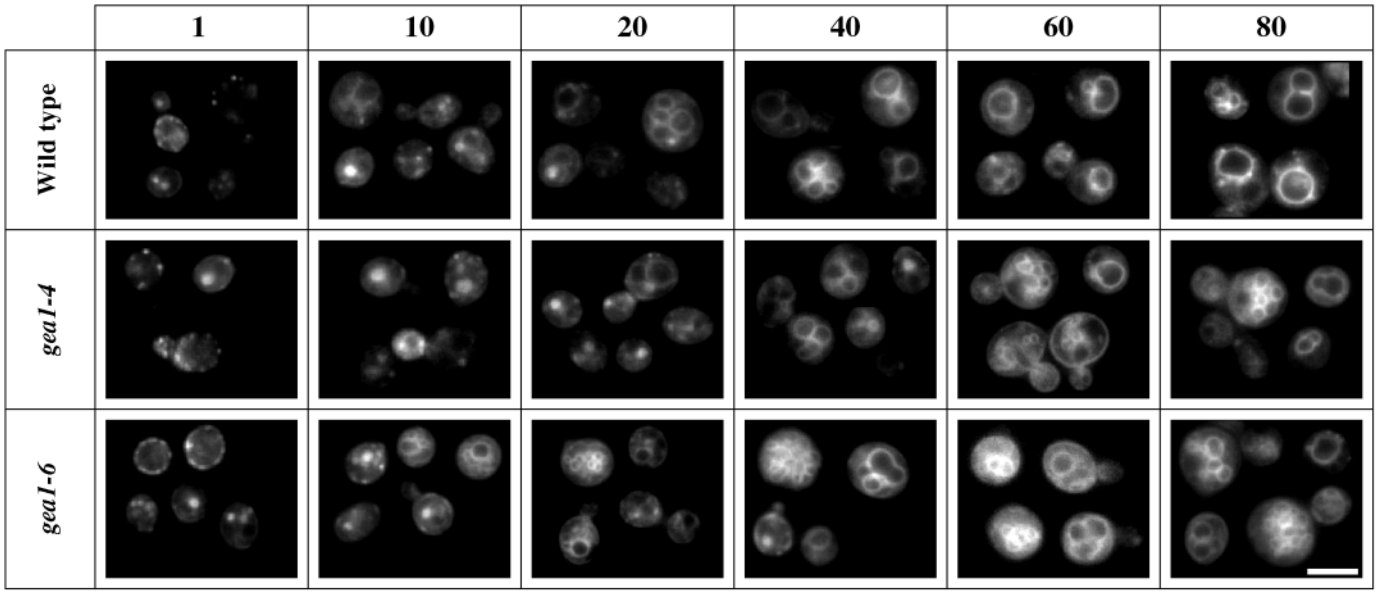


**Fig. 8.** Strains CJY49-3-4 (wildtype), CJY62-10-3 gea1-4 and APY022 *gea1-6* were grown at 24°C, then shifted to 37°C for 10 minutes. Cells were spun down, resuspended in a small volume of medium prewarmed to 37°C, and FM4-64 added at time 0. Cells were incubated at 37°C, and at the time points shown (minutes after addition of FM4-64), cells were removed and fixed with formaldehyde. Bar, 5 μm.

significantly different from that for wild-type cells (Fig. 8). After 40-60 minutes, the majority of cells in wildtype and both mutant populations showed staining in 1-4 vacuolar structures (Fig. 8), although at these late time points, a small percentage (10-20%) of *gea1-4* and *gea1-6* cells showed abnormal patterns of fragmented vacuoles (Fig. 8). These results demonstrate that endocytic and vacuolar structures are not greatly perturbed in the majority of *gea* mutant cells at early time points after shift to the nonpermissive temperature.

### EM analysis of structures accumulated in *gea* mutants

We next examined the ultrastructure of the secretory pathway in wildtype and *gea* mutants by electron microscopy. We used the Karnovsky post-fixation method, followed by counterstaining with thiocarbohydrazide-silver proteinate. This method results in a staining gradient from the more lightly-stained ER/nuclear envelope to the darkly stained cell wall. Relatively thick sections (200 nm) were examined using a stereoscopic approach, which allows a 3D visualization of the elements of the secretory pathway (see Materials and Methods). In wild-type cells, tubular networks were scattered throughout the cytoplasm, as described in the accompanying article (Rambourg et al., 2001). Some of these networks were lightly stained with large, polygonal meshes. Others displayed, at the intersection of narrower meshes, nodular dilations of various sizes and staining intensities that ultimately reached that of secretion granules. In *gea1-4* cells incubated at 37°C, the majority of cells contained large, curved membrane structures made up of tubular networks, many of which had a visible connection to a sheet of unfenestrated ER (Fig. 9A,B). These tubular networks were similar in structure to those found in wild-type cells, and sometimes were seen in proximity to large, darkly stained secretion granules (Fig. 9A,C,D). Similar to BFA-treated cells, tubular networks with narrower meshes and showing nodular dilations of various sizes accumulated in large spherical or ovoid masses (Fig. 9B). In other cases, large-meshed, lightly-stained polygonal networks accumulated in ring-like structures (Fig. 9C, top) or in structures larger than those seen in wild-type cells (Fig. 9D). Ring-like structures made up of narrower-meshed, nodular networks were also observed (Fig. 9E).

The structures that accumulated in *gea1-6* mutant cells after 40 minutes at 37°C were quite different than those found in *gea1-4* cells. Tubular networks, fenestrated membrane structures and secretion granules were rare (Fig. 10). A significant fraction of cells had extensive accumulation of ER membranes (Fig. 10A). The most predominant structures observed were rings, cylinders or spheres of unfenestrated membrane (Fig. 10B,C,D). In some cases, these structures were made up of several stacked layers of membrane (Fig. 10C,D).

## DISCUSSION

The small GTP-binding proteins of the ARF family play a central role in membrane dynamics and protein transport in eukaryotic cells. The GEFs that catalyze GDP/GTP exchange on ARF are of critical importance to ARF function, as they determine when and where ARF proteins will be activated within the cell (reviewed by Jackson and Casanova, 2000). We present here an in vivo characterization of the Gea1p and Gea2p ARF GEFs in the secretory pathway of *S. cerevisiae*. The Gea1p and Gea2p proteins are members of a subfamily of ARF GEFs with members in plants and animals, as well as in yeast (Claude et al., 1999; Steinmann et al., 1999). This subfamily is distinct from that of Sec7p and its mammalian orthologues BIG1 and BIG2 (Mansour et al., 1999; Morinaga et al., 1997; Togawa et al., 1999).

The Gea1p and Gea2p proteins are functionally redundant, but at least one is necessary for viability in yeast. We have generated three temperature-sensitive *gea* mutants and have examined their phenotypes. The *gea1-4* allele carries two substitutions in highly conserved regions of the Sec7 domain, the catalytic domain for ARF nucleotide exchange (Fig. 1), and hence it is likely that the exchange activity of this mutant is compromised in vivo. The *gea1-6* and *gea1-19* alleles, which have very different phenotypes compared with *gea1-4* both structurally and in terms of transport defects, have a wild-type Sec7 domain and lesions in the C-terminal portion of Gea1p. The different *gea* mutants all have certain phenotypes in common. Similar to *arf1Δ* and *arf1-3ts arf2Δ* mutants (Gaynor et al., 1998), the rate of transport of all proteins that continue to be secreted under nonpermissive conditions is decreased in each of the *gea* mutants. However, unlike the *arf* mutants previously characterized, all the *gea* mutants show a cargo-selective secretion defect characteristic of mutants in COPI subunits, such as *sec21-3*. Proteins that continue to be secreted in the *gea* mutants are hypoglycosylated, a phenotype also seen in *arf1Δ*, *arf1-3ts arf2Δ* and *sec21-3* (Gaynor et al., 1998; Gaynor and Emr, 1997). The failure to completely glycosylate proteins is the first observed transport defect in all three *gea* mutants after shift to the nonpermissive temperature. The glycosylation defects in the *gea* mutants are not due to a significant decrease in the steady state level of glycosylation enzymes (at least of the three that we examined: Och1-HA, Anp1p and Mnn1-Myc). Hence Gea1/2p may be involved in activation or regulation of Golgi glycosylation enzyme function, either directly, or indirectly through maintenance of normal Golgi structure (see below).

Of the three *gea* alleles tested, *gea1-4* has the mildest transport defect. The *gea1-6* and *gea1-19* mutants have more severe transport defects, and there is a correspondingly more dramatic effect on structures of the ER-Golgi system. In wild-type yeast cells, Golgi elements correspond to numerous small tubular network structures dispersed in the cytoplasm (see accompanying article; Rambourg et al., 2001). In *gea1-4* mutant cells held at the restrictive temperature, there is a decrease in the number of these tubular network structures, and those that are present are larger than the tubular network structures found in wild-type cells. By contrast, in *gea1-6* and *gea1-19* mutant cells after 40 minutes at the restrictive temperature, very few tubular network or fenestrated membrane structures were seen.

That the tubular networks observed in *gea1-4* mutants by electron microscopy contain Golgi enzymes is supported by immunofluorescence analysis. In *gea1-4* cells, three Golgi enzymes (Och1-HA, Anp1 and Mnn1-Myc) were found in large, ring-like structures whose number per cell was reduced. This result corresponds precisely to the changes in tubular network structures observed by EM, whose size increased and

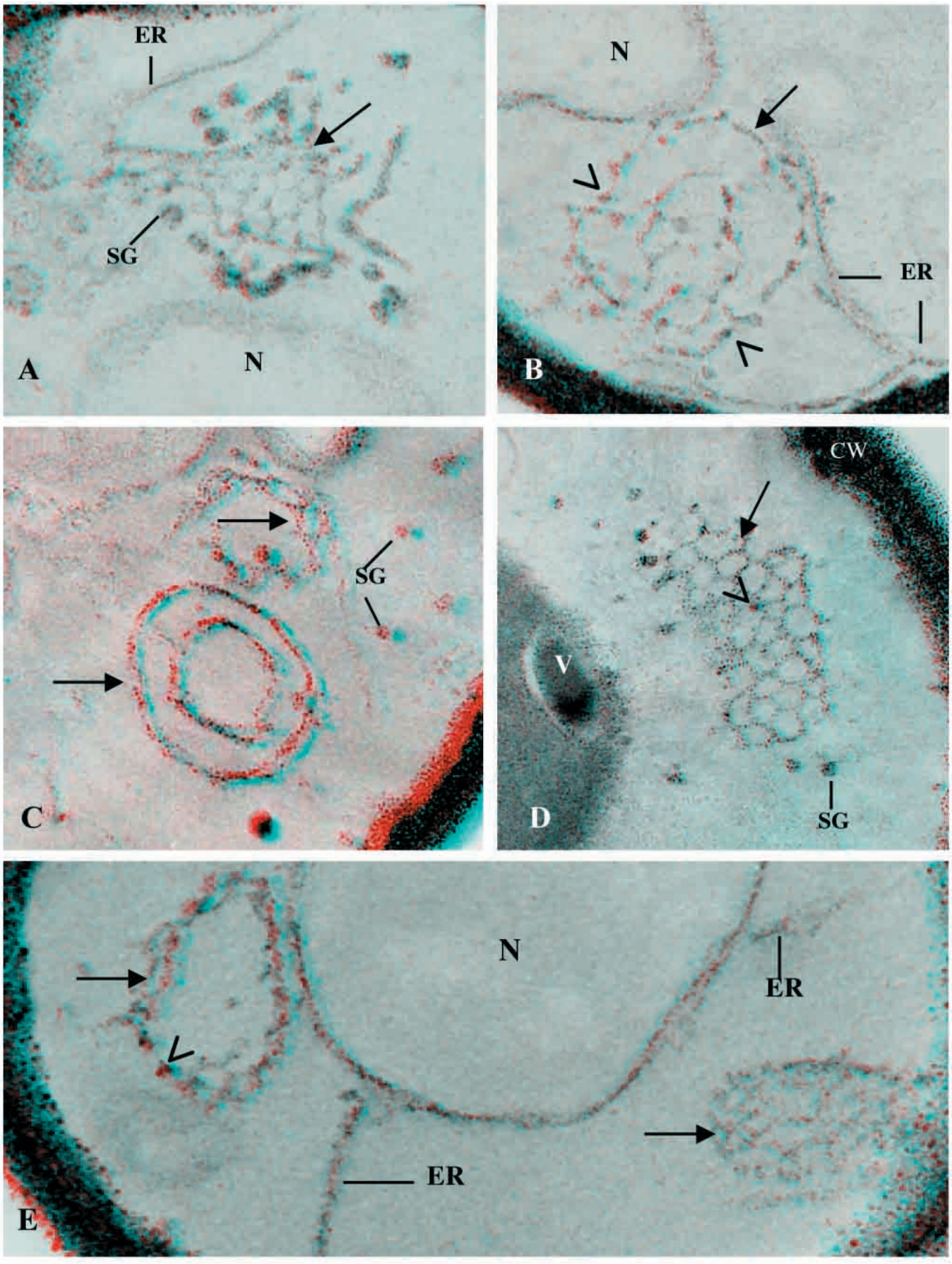
ER
SG
N
A
N
ER
B
SG
C
CW
V
D
SG
N
ER
ER
E

**Fig. 9.** Stereopairs of 0.20 μm thick sections of *gea1-4* mutant cells incubated at 37°C for 40 minutes. (A) A curved tubular network structure (arrow) is connected to an ER sheet (ER; top-left). The central portion consists of a network of wide-meshed, lightly-stained tubules, and at the periphery, larger and more intensely stained tubules display nodules (arrowhead) adjacent to secretion granules (SG). Magnification ×73,500. (B) A large tubular network (arrow) with small dilations at the intersections of polygonal meshes (arrowheads) forms a spherical mass and is connected to an ER ribbon continuous with a sheet of subplasmalemmal ER (ER). N, nucleus. Magnification ×74,500. (C) Tubular networks form ring-like structures (arrows). Wide polygonal meshes are clearly visible in the upper structure, seen in oblique view. Below, fenestrated and tubular structures seen in profile form two concentric rings. SG, secretion granule. Magnification ×87,500. (D) A large, relatively flattened tubular network consists of lightly-stained, wide polygonal meshes (arrow) with a few small dilations (arrowhead). SG, secretion granule; V, vacuole. Magnification ×70,500. (E) A tubular network (arrow, top-left) with darkly stained dilations (arrowhead) forms a ring in proximity to the nuclear envelope. At the bottom-right another tubular network forms a large ovoid mass (arrow). Two ER sheets in continuity with the nuclear envelope are labeled ER. N, nucleus. Magnification ×82,300.

whose number per cell decreased. In *gea1-4* mutants, both the early Golgi enzyme Och1-HA and the late Golgi marker Mnn1-Myc co-localized in the same ring-like structure. This result was also obtained for the rare ring-like structures in *gea1-4* at the permissive temperature of 24°C (Fig. 7B). Hence cis-and trans-Golgi markers in yeast can exist in the same continuous structure.

The large ring-like structures that contain Golgi enzymes that accumulate in *gea1-4* are similar to those that accumulate in the *arf1Δ* and *arf1-3ts arf2Δ* mutants (Gaynor et al., 1998). In these *arf* mutants, endosomes form large ring-like structures as visualized by uptake of the fluorescent dye FM4-64. However, none of the *gea* mutants had this phenotype. For both *gea1-4* and *gea1-6*, endosomal structures visualized by uptake of FM4-64 were indistinguishable from those of the wild-type control. Hence Gea1/2p appears to primarily affect Golgi, rather than endosomal, structure. Since other GEFs for ARF exist in yeast (eg. Sec7p, Syt1p), a plausible hypothesis is that one of these other GEFs is activating ARF in the endosomal pathway followed by FM4-64 to the vacuole.

In the accompanying paper, the structure of the yeast secretory pathway is described. This analysis indicates that an oriented series of membrane transformations starts at the ER, leads to formation of tubular networks and culminates in the liberation of secretion granules. The results of the present paper suggest that the Gea1p and Gea2p ARF GEFs play a role in at least two steps during this series of membrane transformations. The lesion manifest in the *gea1-6* and *gea1-19* mutants is very early and prevents fenestration and tubulization of ER membranes. The lesion in the *gea1-4* mutant occurs at one or multiple points during or after formation of tubular networks and leads to their accumulation. Analysis of the transport defects in *gea1-4* in this and previous work

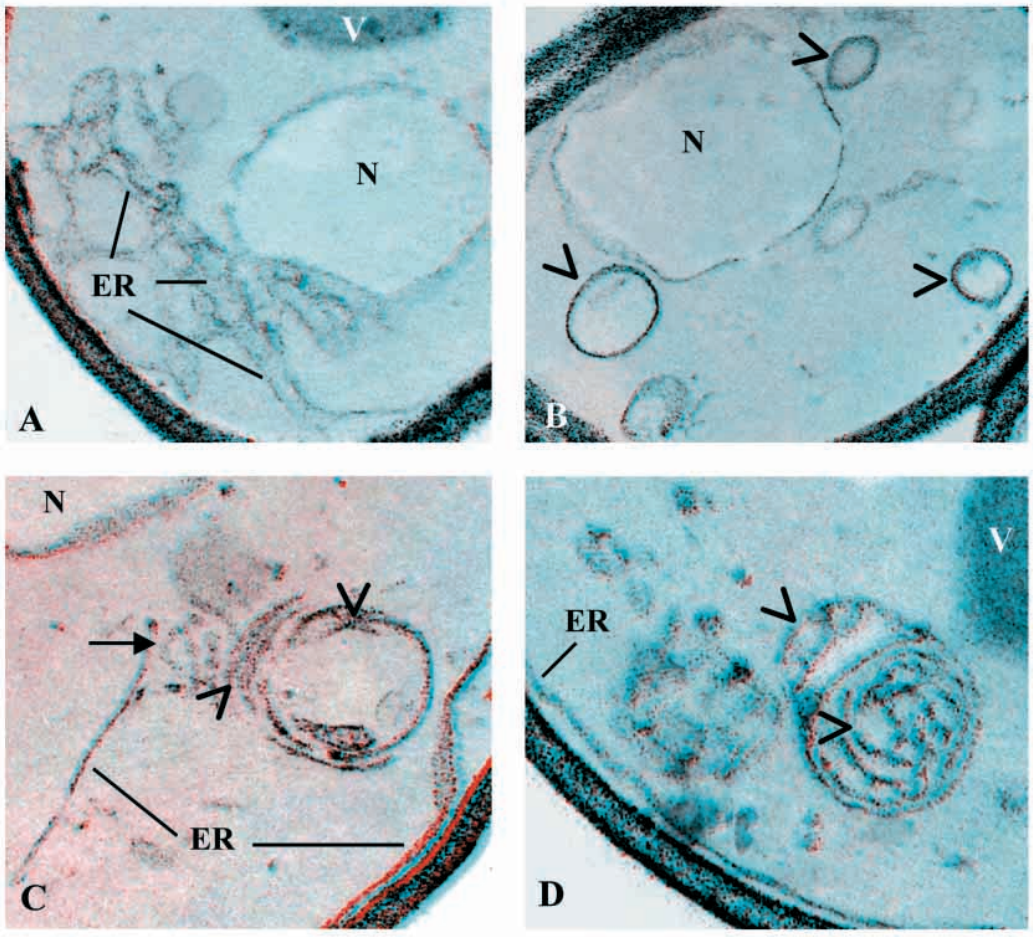


**Fig. 10.** Stereopairs of 0.20 μm thick sections of *gea1-6* mutant cells incubated for 40 minutes at 37°C. (A) Non-fenestrated ER sheets accumulate to form a broad network (ER) interconnecting the nuclear envelope and the subplasmalemmal ER. V, vacuole; N nucleus. Magnification ×36,200. (B) Cylinders or spheres of unfenestrated membrane (arrowheads) are dispersed throughout the cytoplasm. Note the absence of tubular networks and secretory granules. N, nucleus. Magnification ×35,600. (C) A small tubular network (arrow) is continuous on one side with an ER sheet seen in profile, and is continuous on the other side with a multi-layered cylindrical structure (arrowheads). A sheet of unfenestrated ER (ER) is seen in oblique view (bottom-right). N, nucleus. Magnification ×55,600. (D) A cylindrical structure is made up of anastomosed ribbons of unfenestrated membrane (arrowheads). V, vacuole. Magnification ×57,700.

(Peyroche et al., 1996) is consistent with the idea that, in this mutant, transport is slowed at multiple points in transport from the ER to and through the early Golgi.

In summary, we have demonstrated that the Gea1p and Gea2p ARF GEFs, like COPI, are absolutely required for transport of only a subset of proteins through the secretory pathway in *S. cerevisiae*. In *gea* mutants, this subset of cargo proteins was blocked as a heterogeneous population of ER core-glycosylated forms and forms with varying amounts of Golgi glycosylation modifications. Those proteins whose transport was not blocked were secreted at a slower rate and were not fully glycosylated. These transport defects were correlated with profound effects on the structure of the secretory pathway. Immuofluorescence analysis indicated that structures containing both early and late Golgi enzymes were perturbed in the *gea* mutants, and 3D electron microscopy revealed effects of the *gea* lesions on Golgi tubular network structures. These results demonstrate that the Gea1p and Gea2p ARF exchange factors play an important role in maintaining Golgi structure and function in vivo.

We thank Erin Gaynor and Scott Emr for antibodies against CPY, α-pheromone and invertase, and for EGY1213; Randy Schekman for anti-α(1,6)-mannose antiserum and for strain RSY271; Sean Munro for purified anti-Anp1p antibodies and pSDXD1-414 Mnn1-Myc; Marja Makarow for anti-HSP150 antiserum and Gerry Waters for pOH. We also thank Corinne LaMoal for excellent assistance with EM analysis.

## REFERENCES

**Achstetter, T., Franzusoff, A., Field, C. and Schekman, R.** (1988). SEC7 encodes an unusual, high molecular weight protein required for membrane traffic from the yeast Golgi apparatus. *J. Biol. Chem.* **263**, 11711-11717.

**Boman, A. L. and Kahn, R. A.** (1995). Arf proteins: the membrane traffic police? *Trends Biochem. Sci.* **20**, 147-150.

**Busch, M., Mayer, U. and Jürgens, G.** (1996). Molecular analysis of the Arabidopsis pattern formation of gene GNOM: gene structure and intragenic complementation. *Mol. Gen. Genet.* **250**, 681-691.

**Chapman, R. E. and Munro, S.** (1994). The functioning of the yeast Golgi apparatus requires an ER protein encoded by ANP1, a member of a new family of genes affecting the secretory pathway. *EMBO J.* **13**, 4896-4907.

**Chardin, P., Paris, S., Antonny, B., Robineau, S., Béraud-Dufour, S., Jackson, C. L. and Chabre, M.** (1996). A human exchange factor for ARF contains Sec7- and pleckstrin-homology domains. *Nature* **384**, 481-484.

**Claude, A., Zhao, B. P., Kuziemsky, C. E., Dahan, S., Berger, S. J., Yan, J. P., Armold, A. D., Sullivan, E. M. and Melançon, P.** (1999). GBF1. A novel Golgi-associated BFA-resistant guanine nucleotide exchange factor that displays specificity for ADP-ribosylation factor 5. *J. Cell. Biol.* **146**, 71-84.

**Dean, N.** (1999). Asparagine-linked glycosylation in the yeast Golgi. *Biochim. Biophys. Acta* **1426**, 309-322.

**Deitz, S. B., Rambourg, A., Kepes, F. and Franzusoff, A.** (2000). Sec7p Directs the transitions required for yeast Golgi biogenesis. *Traffic* **1**, 172-183.

**Donaldson, J. G., Finazzi, D. and Klausner, R. D.** (1992). Brefeldin A inhibits Golgi membrane-catalysed exchange of guanine nucleotide onto ARF protein. *Nature* **360**, 350-352.

**Franco, M., Chardin, P., Chabre, M. and Paris, S.** (1995). Myristoylation of ADP-ribosylation factor 1 facilitates nucleotide exchange at physiological $Mg^{2+}$ levels. *J. Biol. Chem.* **270**, 1337-1341.

**Franzusoff, A. and Schekman, R.** (1989). Functional compartments of the yeast Golgi apparatus are defined by the sec7 mutation. *EMBO J.* **8**, 2695-2702.

**Franzusoff, A., Redding, K., Crosby, J., Fuller, R. S. and Schekman, R.** (1991). Localization of components involved in protein transport and processing through the yeast Golgi apparatus. *J. Cell Biol.* **112**, 27-37.

**Gaynor, E. C. and Emr, S. D.** (1997). COPI-independent anterograde transport: cargo-selective ER to Golgi protein transport in yeast COPI mutants. *J. Cell Biol.* **136**, 789-802.

**Gaynor, E. C., te Heesen, S., Graham, T. R., Aebi, M. and Emr, S. D.** (1994). Signal-mediated retrieval of a membrane protein from the Golgi to the ER in yeast. *J. Cell Biol.* **127**, 653-665.

**Gaynor, E. C., Chen, C. Y., Emr, S. D. and Graham, T. R.** (1998). ARF is required for maintenance of yeast Golgi and endosome structure and function. *Mol. Biol. Cell* **9**, 653-670.

**Godi, A., Pertile, P., Meyers, R., Marra, P., Di Tullio, G., Iurisci, C., Luini, A., Corda, D. and De Matteis, M. A.** (1999). ARF mediates recruitment of PtdIns-4-OH kinase-beta and stimulates synthesis of PtdIns(4,5)P2 on the Golgi complex. *Nat. Cell Biol.* **1**, 280-287.

**Graham, T. R. and Emr, S. D.** (1991). Compartmental organization of Golgi-specific protein modification and vacuolar protein sorting events defined in a yeast sec18 (NSF) mutant. *J. Cell Biol.* **114**, 207-218.

**Graham, T. R., Seeger, M., Payne, G. S., MacKay, V. L. and Emr, S. D.** (1994). Clathrin-dependent localization of alpha 1,3 mannosyltransferase to the Golgi complex of Saccharomyces cerevisiae. *J. Cell Biol.* **127**, 667-678.

**Harris, S. L. and Waters, M. G.** (1996). Localization of a yeast early Golgi mannosyltransferase, Och1p, involves retrograde transport. *J. Cell Biol.* **132**, 985-998.

**Helms, J. B. and Rothman, J. E.** (1992). Inhibition by brefeldin A of a Golgi membrane enzyme that catalyses exchange of guanine nucleotide bound to ARF. *Nature* **360**, 352-354.

**Honda, A., Nogami, M., Yokozeki, T., Yamazaki, M., Nakamura, H., Watanabe, H., Kawamoto, K., Nakayama, K., Morris, A. J., Frohman, M. A. et al. (**1999). Phosphatidylinositol 4-phosphate 5-kinase alpha is a downstream effector of the small G protein ARF6 in membrane ruffle formation. *Cell* **99**, 521-532.

**Hunziker, W., Whitney, J. A. and Mellman, I.** (1992). Brefeldin A and the endocytic pathway. Possible implications for membrane traffic and sorting. *FEBS Lett.* **307**, 93-96.

**Jackson, C. L. and Casanova, J. E.** (2000). Turning on ARF: the Sec7 family of guanine-nucleotide-exchange factors. *Trends Cell Biol.* **10**, 60-67.

**Jones, S., Jedd, G., Kahn, R. A., Franzusoff, A., Bartolini, F. and Segev, N.** (1999). Genetic interactions in yeast between Ypt GTPases and Arf guanine nucleotide exchangers. *Genetics* **152**, 1543-1556.

**Jungmann, J. and Munro, S.** (1998). Multi-protein complexes in the cis Golgi of Saccharomyces cerevisiae with alpha-1,6-mannosyltransferase activity. *EMBO J.* **17**, 423-434.

**Kirchhausen, T., Bonifacino, J. S. and Riezman, H.** (1997). Linking cargo to vesicle formation: receptor tail interactions with coat proteins. *Curr. Opin. Cell Biol.* **9**, 488-495.

**Klausner, R. D., Donaldson, J. G. and Lippincott-Schwartz, J.** (1992). Brefeldin A: insights into the control of membrane traffic and organelle structure. *J. Cell Biol.* **116**, 1071-1080.

**Klionsky, D. J., Banta, L. M. and Emr, S. D.** (1988). Intracellular sorting and processing of a yeast vacuolar hydrolase: proteinase A propeptide contains vacuolar targeting information. *Mol. Cell. Biol.* **8**, 2105-2116.

**Lippincott-Schwartz, J., Yuan, L. C., Bonifacino, J. S. and Klausner, R. D.** (1989). Rapid redistribution of Golgi proteins into the ER in cells treated with brefeldin A: evidence for membrane cycling from Golgi to ER. *Cell* **56**, 801-813.

**Lupashin, V. V., Kononova, S. V., Ratner Ye, N., Tsiomenko, A. B. and Kulaev, I. S.** (1992). Identification of a novel secreted glycoprotein of the yeast Saccharomyces cerevisiae stimulated by heat shock. *Yeast* **8**, 157-169.

**Mansour, S. J., Skaug, J., Zhao, X. H., Giordano, J., Scherer, S. W. and Melançon, P.** (1999). p200 ARF-GEP1: a Golgi-localized guanine nucleotide exchange protein whose Sec7 domain is targeted by the drug brefeldin A. *Proc. Natl. Acad. Sci. USA* **96**, 7968-7973.

**Morinaga, N., Moss, J. and Vaughan, M.** (1997). Cloning and expression of a cDNA encoding a bovine brain brefeldin A- sensitive guanine nucleotide-exchange protein for ADP-ribosylation factor. *Proc. Natl. Acad. Sci. USA* **94**, 12926-12931.

**Morinaga, N., Tsai, S. C., Moss, J. and Vaughan, M.** (1996). Isolation of a brefeldin A-inhibited guanine nucleotide-exchange protein for ADP ribosylation factor (ARF) 1 and ARF3 that contains a Sec7-like domain. *Proc. Natl. Acad. Sci. USA* **93**, 12856-12860.

**Moss, J. and Vaughan, M.** (1995). Structure and function of ARF proteins: activators of cholera toxin and critical components of intracellular vesicular transport processes. *J. Biol. Chem.* **270**, 12327-12330.

**Orzech, E., Schlessinger, K., Weiss, A., Okamoto, C. T. and Aroeti, B.** (1999). Interactions of the AP-1 Golgi adaptor with the polymeric

immunoglobulin receptor and their possible role in mediating brefeldin A-sensitive basolateral targeting from the trans-Golgi network. *J. Biol. Chem.* **274**, 2201-2215.

**Pearse, B. M., Smith, C. J. and Owen, D. J.** (2000). Clathrin coat construction in endocytosis. *Curr. Opin. Struct. Biol.* **10**, 220-228.

**Peyroche, A., Antonny, B., Robineau, S., Acker, J., Cherfils, J. and Jackson, C. L.** (1999). Brefeldin A acts to stabilize an abortive ARF-GDP-Sec7 domain protein complex: involvement of specific residues of the Sec7 domain. *Mol. Cell* **3**, 275-285.

**Peyroche, A. and Jackson, C. L.** (2000). Functional analysis of ADP-ribosylation factor (arf) guanine nucleotide exchange factors Gea1p and Gea2p in yeast. *Methods Enzymol.* **329**, 290-300.

**Peyroche, A., Paris, S. and Jackson, C. L.** (1996). Nucleotide exchange on ARF mediated by yeast Gea1 protein. *Nature* **384**, 479-481.

**Rambourg, A., Jackson, C. L. and Clermont, Y.** (2001). Three-dimensional configuration of the secretory pathway and segregation of secretion granules in the yeast *Saccharomyces cerevisae*. *J. Cell. Sci.* **114**, 2231-2239.

**Rossanese, O. W., Soderholm, J., Bevis, B. J., Sears, I. B., O'Connor, J., Williamson, E. K. and Glick, B. S.** (1999). Golgi structure correlates with transitional endoplasmic reticulum organization in Pichia pastoris and Saccharomyces cerevisiae. *J. Cell Biol.* **145**, 69-81.

**Russo, P., Kalkkinen, N., Sareneva, H., Paakkola, J. and Makarow, M.** (1992). A heat shock gene from Saccharomyces cerevisiae encoding a secretory glycoprotein. *Proc. Natl. Acad. Sci. USA* **89**, 3671-3675 [published erratum appears in *Proc. Natl. Acad. Sci. USA* (1992) **89**, 8857].

**Schmid, S. L.** (1997). Clathrin-coated vesicle formation and protein sorting: an integrated process. *Annu. Rev. Biochem.* **66**, 511-548.

**Sherman, F., Fink, G. R. and Lawrence, C. W.** (1979). *Methods in Yeast Genetics: A Laboratory Manual.* Cold Spring Harbor, New York: Cold Spring Harbor Laboratory Press.

**Shevell, D. E., Leu, W. M., Gillmor, C. S., Xia, G., Feldmann, K. A. and Chua, N. H.** (1994). EMB30 is essential for normal cell division, cell expansion, and cell adhesion in Arabidopsis and encodes a protein that has similarity to Sec7. *Cell* **77**, 1051-1062.

**Springer, S., Spang, A. and Schekman, R.** (1999). A primer on vesicle budding. *Cell* **97**, 145-148.

**Steinmann, T., Geldner, N., Grebe, M., Mangold, S., Jackson, C. L., Paris, S., Gälweiler, L., Palme, K. and Jürgens, G.** (1999). Coordinated polar localization of auxin efflux carrier PIN1 by GNOM ARF GEF. *Science* **286**, 316-318.

**Togawa, A., Morinaga, N., Ogasawara, M., Moss, J. and Vaughan, M.** (1999). Purification and cloning of a brefeldin A-inhibited guanine nucleotide- exchange protein for ADP-ribosylation factors. *J. Biol. Chem.* **274**, 12308-12315.

**Vida, T. A. and Emr, S. D.** (1995). A new vital stain for visualizing vacuolar membrane dynamics and endocytosis in yeast. *J. Cell Biol.* **128**, 779-792.

**Wieland, F. and Harter, C.** (1999). Mechanisms of vesicle formation: insights from the COP system. *Curr. Opin. Cell Biol.* **11**, 440-446.

**Wood, S. A. and Brown, W. J.** (1992). The morphology but not the function of endosomes and lysosomes is altered by brefeldin A. *J. Cell. Biol.* **119**, 273-285.

**Yan, J. P., Colon, M. E., Beebe, L. A. and Melançon, P.** (1994). Isolation and characterization of mutant CHO cell lines with compartment-specific resistance to brefeldin A. *J. Cell. Biol.* **126**, 65-75.